

# Pressure-induced phase transitions in the multiferroic perovskite $\text{BiFeO}_3$ studied by far-infrared micro-spectroscopy

A. Pashkin, K. Rabia, S. Frank, and C. A. Kuntscher\*  
*Experimentalphysik 2, Universität Augsburg, D-86135 Augsburg, Germany*

R. Haumont and R. Saint-Martin  
*Laboratoire de Physico-Chimie de l'Etat Solide (CNRS), Université Paris XI, 91405 Orsay, France*

J. Kreisel  
*Laboratoire Matériaux et Génie Physique (CNRS),  
 Grenoble Institute of Technology, 38016 Grenoble, France*  
 (Dated: February 9, 2022)

We present the results of pressure-dependent far-infrared reflectivity measurements on the multiferroic perovskite  $\text{BiFeO}_3$  at room temperature. The observed behavior of the infrared-active phonon modes as a function of pressure clearly reveals two structural phase transitions around 3.0 and 7.5 GPa, supporting the results of recent Raman and x-ray diffraction studies under pressure. Based on the pressure-dependent frequency shifts of the infrared-active phonon modes we discuss the possible character of the phase transitions.

PACS numbers: 77.80.-e, 75.50.Ee, 78.30.-j, 62.50.-p

## I. INTRODUCTION

The perovskite  $\text{BiFeO}_3$  is a robust magnetoelectric multiferroic,<sup>1,2</sup> with the coexistence of ferroelectric and antiferromagnetic order up to unusually high temperatures.  $\text{BiFeO}_3$  bulk samples exhibit an antiferromagnetic Néel temperature of  $\sim 370^\circ\text{C}$  and a ferroelectric Curie temperature of  $\sim 830^\circ\text{C}$ .<sup>3,4</sup> For possible applications the growth of high-quality thin films and the study of their physical properties are of major interest. It is known that the properties of multiferroic thin films can be significantly altered by the lattice mismatch between the material and the substrate.<sup>5,6,7,8</sup> The enhanced ferroelectric polarization in  $\text{BiFeO}_3$  films<sup>5,7</sup> compared to bulk material were initially proposed to be driven by epitaxial strain; this matter is, however, controversially debated.<sup>9,10,11,12</sup> Recently a high spontaneous polarization value - close to theoretical predictions<sup>13,14</sup> - has been also reported for high-quality  $\text{BiFeO}_3$  ceramics<sup>15</sup> and single crystals,<sup>16,17</sup> demonstrating that a large spontaneous polarization is an intrinsic property of  $\text{BiFeO}_3$  bulk samples and probably not induced by a strain.

In general,  $\text{BiFeO}_3$  is a complex system with magnetic, ferroelectric and ferroelastic order parameters which are mutually coupled. Thus, various instabilities can be driven by external thermodynamical variables, like temperature, pressure, electric or magnetic field, resulting in a particularly rich phase diagram. Experimental<sup>18,19,20,21</sup> and theoretical<sup>14</sup> investigations have investigated the influence of external pressure on  $\text{BiFeO}_3$ . In fact, the importance of high-pressure studies was demonstrated for a number of ferroelectric materials.<sup>22,23,24,25,26</sup> *Ab initio* calculations of the total energy for different structural arrangements of  $\text{BiFeO}_3$  suggest that at pressures above 13 GPa the  $Pnma$  phase

possesses lower energy than the  $R3c$  phase.<sup>14</sup> Thus, a pressure-induced structural phase transition from the polar rhombohedral  $R3c$  structure to the nonpolar orthorhombic  $Pnma$  structure was predicted. Pressure-dependent Raman and x-ray diffraction studies carried out on  $\text{BiFeO}_3$  single crystals<sup>18,19</sup> indeed revealed two pressure-induced structural phase transitions at around 3 and 10 GPa. The first phase transition at  $P_{c1} \approx 3$  GPa was assigned to a distortion of the  $\text{BiFeO}_3$  rhombohedral unit cell; however, the exact character of the structural changes could not be determined yet. The second phase transition at  $P_{c2} \approx 10$  GPa is most probably related to a suppression of the cation displacements (with a concomitant suppression of the ferroelectricity), and it was proposed that the crystal structure changes from rhombohedral  $R3c$  to orthorhombic  $Pnma$ , in good agreement with recent *ab-initio* calculations<sup>14</sup> (although the experimental work suggests an intermediate bridging phase).

The low pressure of the first phase transition ( $\approx 3$  GPa) in bulk  $\text{BiFeO}_3$  indicates a high sensitivity of the system regarding stress and may originate from a complex interplay between the magnetic, ferroelectric and ferroelastic order parameters. Furthermore, experimental studies at very high pressures<sup>20,21</sup> (up to 70 GPa) have revealed a transition from an antiferromagnetic to a nonmagnetic state at 47 GPa. In the same pressure range  $\text{BiFeO}_3$  undergoes an insulator-to-metal transition evidenced by optical and transport measurements.<sup>21</sup>

Until now the reported far-infrared reflectivity measurements on  $\text{BiFeO}_3$  addressed only the temperature dependence of the phonon response. Kamba et al.<sup>27</sup> reported far-infrared reflectivity spectra of  $\text{BiFeO}_3$  ceramics in a broad temperature range (20 - 950 K) and discovered a softening of some phonon modes on approaching the ferroelectric transition temperature. Recently, far-infrared spectra of single crystals<sup>16,17</sup> between 5 K and

300 K have been presented by Lobo et al.<sup>28</sup> with careful assignment of the phonon modes and analysis of their contribution to the static dielectric constant.

In this paper we report the effect of pressure on the far-infrared response of BiFeO<sub>3</sub> single crystals at room temperature. Reflectivity spectra of single-crystal samples were measured using far-infrared micro-spectroscopy in combination with a diamond anvil high pressure cell. The primary motivation of our investigations was to confirm the recently found structural phase transitions under high pressure and to obtain additional information about their character.

In general, high-pressure infrared studies of phonon modes are rare in the literature, mainly because of the experimental difficulties when compared with Raman scattering. To the best of our knowledge, the present work is the first systematic study of the phonon behavior in ferroelectrics under high pressure by means of infrared reflection spectroscopy.

## II. EXPERIMENT

The investigated BiFeO<sub>3</sub> single crystals were grown using a Fe<sub>2</sub>O<sub>3</sub>/Bi<sub>2</sub>O<sub>3</sub> (1:4 M ratio) flux in a platinum crucible. The flux was held at 920°C and slowly cooled, similarly to the previously reported procedure.<sup>29</sup> Light yellow translucent crystals in a shape of thin platelets have been isolated by dissolving the flux in dilute nitric acid. Back-reflection Laue photographs indicate a (001)<sub>pc</sub> crystallographic orientation of the platelets (where the index *pc* denotes a pseudo-cubic setting). X-ray diffraction measurements performed on crushed crystals reveal a pure perovskite phase free from secondary phases.

Pressure-dependent far-infrared reflectivity measurements at room temperature were carried out at the infrared beamline of the synchrotron radiation source ANKA in Karlsruhe using a Bruker IFS 66v/S Fourier transform infrared spectrometer. A diamond anvil cell equipped with type IIA diamonds suitable for infrared measurements was used to generate pressures up to 14.4 GPa. To focus the infrared beam onto the small sample in the pressure cell, a Bruker IR Scope II infrared microscope with a 15x magnification objective was used.

The measurement of the infrared reflectivity has been performed on the surface of as-grown BiFeO<sub>3</sub> crystals. A small piece of sample (about 80 μm × 80 μm × 40 μm) was placed in the hole (150 μm diameter) of a steel gasket. With this crystal size and the corresponding diffraction limit, we were able to measure reliably the frequency range above 200 cm<sup>-1</sup>. Finely ground CsI powder was added as a quasi-hydrostatic pressure-transmitting medium. The ruby luminescence method<sup>30</sup> was used for the pressure determination.

Reflectivity spectra were measured at the interface between sample and diamond. The measurement geometry is shown in the inset of Fig. 1. Spectra taken at the inner diamond-air interface of the empty cell served

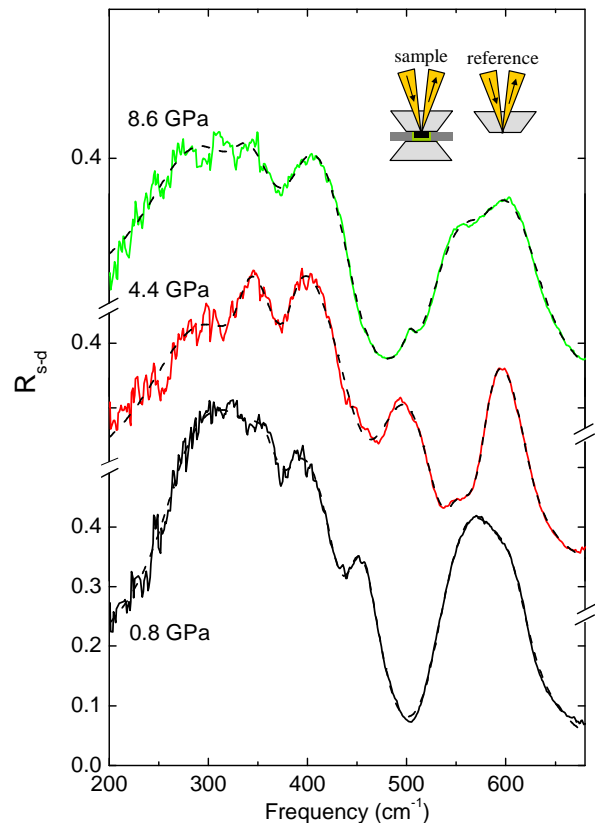


FIG. 1: (Color online) Room-temperature reflectivity  $R_{s-d}$  spectra of BiFeO<sub>3</sub> for three selected pressures (0.8, 4.4, 8.6 GPa); the spectra are offset along the vertical axis for clarity. The dashed lines are the fits with the generalized-oscillator model according to Eq. (1) (see text for details). Inset: Measurement geometry for the reflectivity measurements, as described in the text.

as the reference for normalization of the sample spectra. The absolute reflectivity at the sample-diamond interface, denoted as  $R_{s-d}$ , was calculated according to  $R_{s-d}(\omega) = R_{dia} \times I_s(\omega)/I_d(\omega)$ , where  $I_s(\omega)$  denotes the intensity spectrum reflected from the sample-diamond interface and  $I_d(\omega)$  the reference spectrum of the diamond-air interface.  $R_{dia} = 0.167$  was calculated from the refractive index of diamond,  $n_{dia} = 2.38$ , and assumed to be independent of pressure. This is justified because  $n_{dia}$  is known to change only very little with pressure.<sup>31,32</sup> Variations in synchrotron source intensity were taken into account by applying additional normalization procedures. The reproducibility was ensured by two experimental runs on different crystals.

The presented high pressure spectra were collected without polarizer, since synchrotron radiation is strongly polarized by itself. The orientation of the samples in the pressure cell allowed us to probe the response of the phonon modes polarized normal to the direction of spontaneous polarization, similar to Ref.28 (as discussed in Section III).

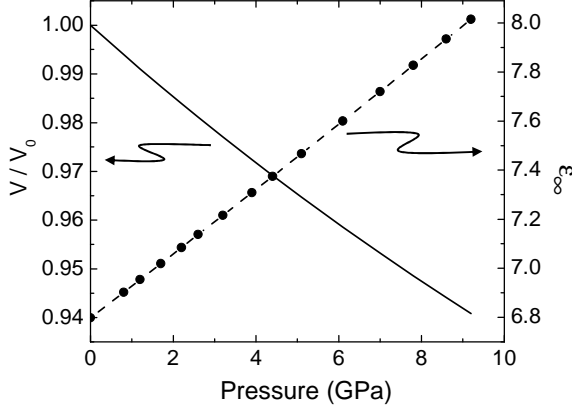


FIG. 2: Pressure dependence of the unit cell volume, calculated according to the first order Birch equation of state [Eq. (5)] and the high-frequency permittivity  $\epsilon_\infty$  as a function of pressure, calculated according to the Clausius-Mossotti relation [Eq. (4)].

### III. RESULTS

In Fig. 1 we show the far-infrared reflectivity spectra of BiFeO<sub>3</sub> at room-temperature for three selected pressures; the spectra are offset along the vertical axis for clarity. Following the analysis of the infrared and terahertz spectra in Ref.27, we applied to our spectra the generalized-oscillator model with the factorized form of the complex dielectric function:<sup>33</sup>

$$\epsilon(\omega) = \epsilon_\infty \prod_{j=1}^n \frac{\omega_{LO_j}^2 - \omega^2 + i\omega\gamma_{LO_j}}{\omega_{TO_j}^2 - \omega^2 + i\omega\gamma_{TO_j}}, \quad (1)$$

where  $\omega_{TO_j}$  and  $\omega_{LO_j}$  denote the transverse and longitudinal frequencies of the  $j$ th polar phonon mode, respectively, and  $\gamma_{TO_j}$  and  $\gamma_{LO_j}$  denote their corresponding damping constants. The oscillator strength  $\Delta\epsilon_j$  [i.e., contribution of the phonon mode to the static dielectric constant  $\epsilon(0)$ ] of the  $j$ th polar phonon can be calculated from the formula<sup>33</sup>

$$\Delta\epsilon_j = \frac{\epsilon_\infty}{\omega_{TO_j}^2} \frac{\prod_k (\omega_{LO_k}^2 - \omega_{TO_j}^2)}{\prod_{k \neq j} (\omega_{TO_k}^2 - \omega_{TO_j}^2)}. \quad (2)$$

The four-parameter oscillator model [Eq. (1)] follows from the general properties of the dielectric function in a polarizable lattice (pole at transverse and zero at longitudinal eigenfrequencies of polar phonons) and it is able to describe the permittivity of dielectrics in most cases. However, it has a drawback since a certain combination of parameter values in Eq. (1) may result in unphysical values of the complex permittivity<sup>33,34</sup> (for example, negative losses or finite conductivity at infinite frequency). Therefore, in our fitting procedure of the infrared reflectivity we restricted the parameter values to those which result in an optical conductivity vanishing at frequencies much higher than the phonon eigenfrequencies.

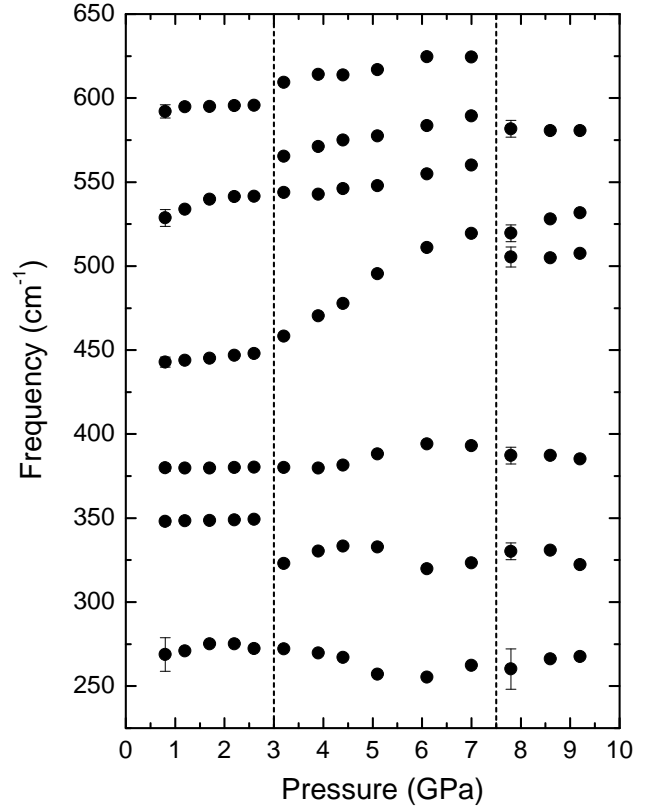


FIG. 3: Frequencies of the transverse optical phonons in BiFeO<sub>3</sub> as a function of pressure, obtained by fitting the reflectivity spectra  $R_{s-d}(\omega)$  with the generalized-oscillator model. The vertical dashed lines indicate the pressures of the two phase transitions.

The dielectric function  $\epsilon(\omega)$  [Eq. (1)] is directly related to the measured reflectivity  $R_{s-d}(\omega)$  at the sample-diamond interface by the Fresnel equation

$$R_{s-d}(\omega) = \left| \frac{\sqrt{\epsilon(\omega)} - n_{\text{dia}}}{\sqrt{\epsilon(\omega)} + n_{\text{dia}}} \right|^2. \quad (3)$$

The pressure dependence of the high-frequency permittivity  $\epsilon_\infty$  used in our fitting was calculated according to the Clausius-Mossotti relation:<sup>35</sup>

$$\frac{\epsilon_\infty(P) - 1}{\epsilon_\infty(P) + 2} = \frac{\alpha}{3\epsilon_0 V(P)}, \quad (4)$$

where  $\alpha$  is the electronic polarizability of the unit cell, which was obtained from the lowest-pressure data. The pressure dependence of the unit cell volume,  $V(P)$ , has not been measured yet; therefore we calculated  $V(P)$  according to the first-order Birch equation of state:<sup>36</sup>

$$P(x) = \frac{3}{2} B_0 x^{-7} (1 - x^2), \quad (5)$$

where  $x = [V(P)/V(0)]^{1/3}$ . For the bulk modulus at zero pressure we assumed  $B_0 = 130.9$  GPa according to the ab-initio calculations.<sup>14</sup> The resulting pressure dependence

TABLE I: Room-temperature fitting parameters from Eq. (1) to describe the reflectivity spectrum of BiFeO<sub>3</sub> at 0.8 GPa, compared to the room-temperature parameters obtained at ambient pressure by Lobo et al.,<sup>28</sup> denoted by  $\omega_{TO}^{amb}$ ,  $\gamma_{TO}^{amb}$  and  $\Delta\epsilon^{amb}$ .

$\omega_{TO}(\gamma_{TO})$	$\omega_{TO}^{amb}(\gamma_{TO}^{amb})$	$\omega_{LO}(\gamma_{LO})$	$\Delta\epsilon$	$\Delta\epsilon^{amb}$
269 (51)	262 (9.1)	348 (41)	18.2	14.8
	274 (33.5)			2.45
348 (36)	340 (17.4)	374 (43)	0.023	0.27
380 (41)	375 (21.6)	433 (43)	0.32	0.475
443 (33)	433 (33.8)	472 (44)	0.15	0.301
529 (48)	521 (41.3)	588 (48)	0.69	1.14
592 (46)		614 (37)	0.019	

of the unit cell volume is presented in Fig. 2 together with the high-frequency permittivity  $\epsilon_\infty$  as a function of pressure, calculated with Eq. (4). The estimated value of  $\epsilon_\infty$  at ambient pressure is 6.8. It is higher than the value of 4.0 reported for BiFeO<sub>3</sub> ceramics,<sup>27</sup> however, lower than  $\epsilon_\infty = 9.0$  reported for single crystals.<sup>28</sup> Therefore, the  $\epsilon_\infty$  value used in this work is reasonable. However, its precision is critically dependent on several parameters which can hardly be controlled in pressure experiments (like surface quality, parasitic reflections from diamond anvil interfaces etc.).

The reflectivity spectra could be well fitted with the generalized-oscillator model according to Eq. (1). As examples, we show in Fig. 1 the reflectivity spectra  $R_{s-d}$  of BiFeO<sub>3</sub> at three selected pressures and the corresponding fits with the generalized-oscillator model. Below  $P_{c1} = 3$  GPa the reflectivity spectra in the measured frequency range can be well fitted using 6 oscillator terms. Above 3 GPa an additional oscillator term is needed for a reasonable fit of the spectra. Finally, above 7.5 GPa the number of oscillators reduces to six again. The pressure dependence of the transverse phonon frequencies is shown in Fig. 3.

The factor-group analysis predicts 13 infrared- and Raman-active phonon modes for the room temperature  $R3c$  phase of BiFeO<sub>3</sub>. They can be classified according to the irreducible representations  $4A_1 + 9E$ , i.e., there are 4  $A_1$  modes polarized along the direction of the spontaneous polarization and 9  $E$  doublets polarized normal to this direction. In addition, there are 5  $A_2$  silent modes. The frequencies of the optical phonons have been calculated theoretically<sup>37</sup> and determined experimentally by infrared<sup>28</sup> and Raman<sup>38,39</sup> spectroscopy on single BiFeO<sub>3</sub> crystals. According to the fit of our data with the generalized-oscillator model the transverse optical modes are located at 269, 348, 380, 443, 529 and 592 cm<sup>-1</sup> for the lowest measured pressure (0.8 GPa). In Table I we list the frequencies of the transverse and longitudinal optical modes obtained by our infrared reflectivity measurements on single crystals at the lowest pressure together with the ambient-pressure results for

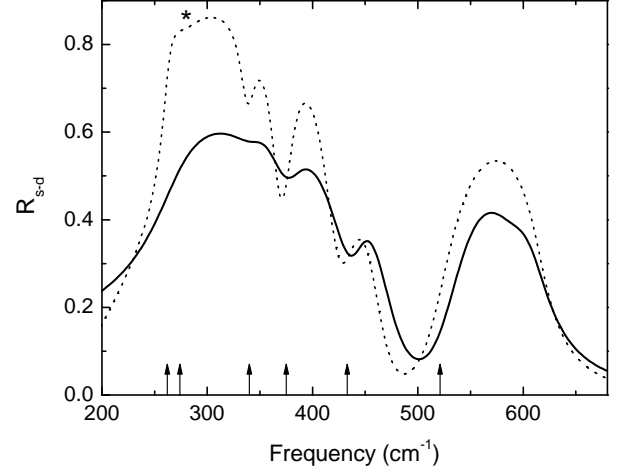


FIG. 4: Fit of the measured reflectivity spectrum of BiFeO<sub>3</sub> at 0.8 GPa (solid line) compared to the simulated ambient pressure spectrum in the diamond anvil cell using the fitting parameters from Ref.28 (dashed line). The arrows indicate the frequencies of TO phonons found by Lobo et al.<sup>28</sup> The asterisk marks the kink produced by the mode at 274 cm<sup>-1</sup>.

BiFeO<sub>3</sub> single crystal obtained by Lobo et al.<sup>28</sup> There is a very good agreement between the transverse phonon frequencies  $\omega_{TO}$  and  $\omega_{TO}^{amb}$ . However, the damping constants  $\gamma_{TO}$  are higher in the case of our pressure measurements. The difference in the far-infrared reflectivity spectra  $R_{s-d}(\omega)$  for the two sets of parameters given in Table I is illustrated in Fig. 4. Obviously, both reflectivity spectra look similar and differ only in the overall reflectivity level and the sharpness of the phonon dips. The broadening of the phonon modes under high pressure is rather common: it is related to the increase of the number of lattice defects in the sample under pressure application, resulting in an increase of the phonon scattering rate. Perhaps the mode at 274 cm<sup>-1</sup> which produces a small dip in the reflectivity curve (marked by an asterisk in Fig. 4) observed by Lobo et al. becomes even weaker due to the broadening effect in our pressure measurements. Thus, it could not be reliably resolved in the measured spectra and was therefore neglected in our fitting procedure.

All the phonon modes listed in Table I, besides the weak mode at 592 cm<sup>-1</sup>, belong to the  $E$  representation, i.e., they are polarized perpendicular to the direction of spontaneous polarization  $[111]_{pc}$ . This indicates that the electric field of the synchrotron radiation used in our experiment was polarized approximately along the  $[-110]_{pc}$  direction, similar to the experiment of Lobo et al.<sup>28</sup>

The evolution of the optical conductivity  $\sigma'(\omega) = \omega\epsilon_0\epsilon''(\omega)$  with increase of pressure is shown in Fig. 5. One can clearly see the drastic changes of the optical conductivity spectra across the transition pressures  $P_{c1} = 3$  GPa and  $P_{c2} = 7.5$  GPa.

#### IV. DISCUSSION

The five detected phonon modes can be assigned to the bending and stretching modes of the  $\text{FeO}_6$  octahedra, which exhibit a displacement of the  $\text{Fe}^{3+}$  cations from their centrosymmetric position along the pseudo-cubic  $[111]_{pc}$  direction.<sup>29,40</sup> The change in the pressure dependence of the phonon mode frequencies at  $P_{c1}$  and  $P_{c2}$  could thus be assigned to changes in the octahedral distortion. By comparison with the phonon spectra of typical perovskite materials like  $\text{LaTiO}_3$  and  $\text{BaTiO}_3$ ,<sup>41,42</sup> the experimentally observed modes can be attributed to  $\text{FeO}_6$  octahedral bending and stretching modes (in the frequency ranges  $200\text{--}400\text{ cm}^{-1}$  and  $400\text{--}850\text{ cm}^{-1}$ , respectively). The Bi ions are involved only in the lower-frequency ( $<200\text{ cm}^{-1}$ ) modes located below the measured frequency range of this study.

Recent pressure-dependent Raman and x-ray diffraction studies revealed two pressure-induced structural phase transitions at around 3 and 10 GPa:<sup>18,19</sup> The phase transition at 3 GPa was interpreted in terms of a change of the cation displacement and the octahedral tilting. At 10 GPa a suppression of the cation displacements (with a concomitant suppression of the ferroelectricity) and a change of the crystal symmetry to orthorhombic  $Pnma$ , was suggested to occur. The second phase transition is in agreement with ab-initio calculations<sup>14</sup> which predict a pressure-induced change of the crystal symmetry to the  $Pnma$  group at around 13 GPa.

Our pressure-dependent far-infrared data confirm the occurrence of two phase transitions in  $\text{BiFeO}_3$ . In particular, we can confirm the phase transition at  $P_{c1} \approx 3$  GPa, which is surprisingly low considering the robustness of the ferroelectricity in  $\text{BiFeO}_3$  with respect to the temperature increase. The high spontaneous electrical polarization observed also for strained  $\text{BiFeO}_3$  thin films,<sup>5,6,7</sup> where the stress induced by the mismatch between film and substrate is comparable to the compressive stress produced by external pressure<sup>18</sup> around  $P_{c1}$ , suggests that the symmetry of the crystal above 3 GPa can be still described by a polar space group, although different from the ambient-pressure  $R3c$  group. Among possible candidates are the tetragonal  $P4mm$  and the monoclinic  $Cm$  groups suggested for epitaxial thin films,<sup>43,44</sup> which are energetically close to the  $R3c$  structure according to ab-initio calculations.<sup>14</sup> The most remarkable signature of the phase transition at 3 GPa is the appearance of a phonon mode at  $565\text{ cm}^{-1}$  (see Figs. 3 and 5). Furthermore, the pressure dependence of the frequency of the other TO phonon modes demonstrates anomalies across the transition pressure (change of the slope of the frequency shift). In contrast to this finding, the Raman measurements under pressure detected the appearance of new modes and clear anomalies around 3 GPa only for the modes below  $250\text{ cm}^{-1}$  which were not accessible by our far-infrared study. We speculate that the new Raman and infrared modes originate from the silent  $A_2$  modes of the parental  $R3c$  phase which become active

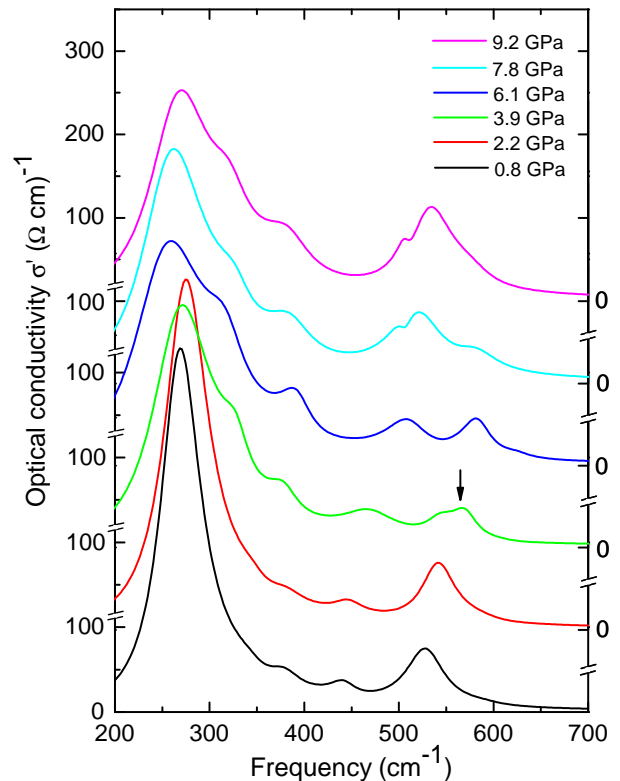


FIG. 5: (Color online) Real part  $\sigma'(\omega)$  of the optical conductivity of  $\text{BiFeO}_3$  for selected pressures, obtained by fitting the reflectivity spectra  $R_{s-d}(\omega)$  with the generalized-oscillator model; the spectra are offset along the vertical axis for clarity. The arrow marks the position of the phonon mode at  $565\text{ cm}^{-1}$  emerging above 3 GPa.

due to symmetry change above 3 GPa. Since the activated phonon modes appear in the frequencies ranges typical for oxygen octahedra stretching modes as well as for modes involving vibration of the Bi ions, we conclude that the crystal structure change at  $P_{c1}$  is characterized by the simultaneous tilting of oxygen octahedra and the Bi cations displacement.

At higher pressures a second transition into the paraelectric phase with  $Pnma$  symmetry has been predicted theoretically<sup>14</sup> at 13 GPa, and it was observed experimentally by Raman spectroscopy and x-ray diffraction<sup>18,19</sup> at about 10 GPa. Since the unit cell of the orthorhombic perovskite with  $Pnma$  space group contains 4 formula units,<sup>45</sup> i.e., twice more atoms than the rhombohedral  $R3c$  unit cell of the  $\text{BiFeO}_3$ , the number of the phonon modes should double in the paraelectric phase. However, due to the exclusion rule which applies to all crystals with inversion symmetry, the Raman and infrared-active modes belong to different symmetry species. In analogy with the perovskite  $\text{LaMnO}_3$ ,<sup>45</sup> there should be in total 25 infrared modes ( $9B_{1u} + 7B_{2u} + 9B_{3u}$ ) and 24 Raman modes ( $7A_g + 5B_{1g} + 7B_{2g} + 5B_{3g}$ ) in the paraelectric phase of  $\text{BiFeO}_3$ . The increased num-

ber of modes in the  $Pnma$  phase compared to 13 modes in the  $R3c$  phase should originate from the splitting of the  $E$  symmetry doublets and the general doubling of all modes due to the unit cell doubling. Thus, one would expect to observe a splitting of the phonon modes across the transition pressure, although some modes can vanish due to the selection rules. Such effects were reported in pressure-dependent Raman measurements of  $\text{BiFeO}_3$  crystals around 9-10 GPa.<sup>19</sup> Our infrared measurements demonstrate a similar effect: above 7.5 GPa the mode at  $520\text{ cm}^{-1}$  splits into two modes (see Figs. 3, 5). On the other hand, two of the infrared modes above  $550\text{ cm}^{-1}$  cannot be resolved above 7.5 GPa possibly as a result of exclusion rule in the centrosymmetric  $Pnma$  phase. Thus, our infrared study confirms the pressure-induced transition into the paraelectric phase. However, the transition pressure  $P_{c2} \simeq 7.5\text{ GPa}$  is somewhat lower than the value of 9-10 GPa reported from x-ray diffraction and Raman studies.<sup>18,19</sup> This difference in pressure can be understood by the different pressure transmitting media used in the two experimental investigations (argon in the earlier measurements<sup>18,19</sup> and CsI in our case), since under more hydrostatic conditions (argon) the transition is expected to occur at *higher* pressure.<sup>46</sup>

## V. SUMMARY

We have studied the far-infrared reflectivity of the multiferroic material  $\text{BiFeO}_3$  under high pressure. The fre-

quencies of the transverse optical phonons demonstrate two distinct anomalies in their pressure dependence at 3.0 and 7.5 GPa, which can be assigned to structural phase transitions. The results of our infrared spectroscopy study are in good agreement with recent Raman and x-ray diffraction studies under pressure.<sup>18,19</sup> The analysis of the phonon behavior suggests that the transition at 3 GPa is characterized by the simultaneous tilting of oxygen octahedra and the Bi cations displacement. The changes across 7.5 GPa are consistent with a transition into the paraelectric  $Pnma$  phase predicted theoretically<sup>14</sup> and observed experimentally by a recent x-ray diffraction study.<sup>19</sup>

## Acknowledgements

We acknowledge the ANKA Angströmquelle Karlsruhe for the provision of beamtime and we would like to thank B. Gasharova, Y.-L. Mathis, D. Moss, and M. Süpfle for assistance using the beamline ANKA-IR. Financial support by the Bayerische Forschungsförderung and the DFG through the SFB 484 is gratefully acknowledged. Support from the French National Research Agency (ANR Blanc) is greatly acknowledged by RH and JK. JK thanks the European network of excellence FAME and the European STREP MaCoMuFi for financial support.

- 
- \* E-mail: christine.kuntscher@physik.uni-augsburg.de
- <sup>1</sup> G. A. Smolenskii and I. Chupis, *Sov. Phys. Usp.* **25**, 475 (1982).
  - <sup>2</sup> M. Fiebig, *J. Phys. D* **38**, R123 (2005).
  - <sup>3</sup> S. V. Kielev, R. P. Ozerov, and G. S. Zhdanov, *Sov. Phys. Dokl.* **7**, 742 (1963).
  - <sup>4</sup> G. A. Smolenskii, V. A. Isupov, A. I. Agranovskaya, and N. N. Krainik, *Sov. Phys. Sol. Stat.* **2**, 2651 (1961).
  - <sup>5</sup> J. Wang, J. B. Neaton, H. Zheng, V. Nagarajan, S. B. Ogale, B. Liu, D. Viehland, V. Vaithyanathan, D. G. Schlom, U. V. Waghmare, N. A. Spaldin, K. M. Rabe, M. Wuttig, and R. Ramesh, *Science* **299**, 1719 (2003).
  - <sup>6</sup> K. Y. Yun, D. Ricinschi, T. Kanashima, M. Noda, and M. Okuyama, *Jpn. J. Appl. Phys. Part 2* **43**, L647 (2004).
  - <sup>7</sup> J. Li, J. Wang, M. Wuttig, R. Ramesh, N. Wang, B. Ruetter, A. P. Pyatakov, A. K. Zvezdin, and D. Viehland, *Appl. Phys. Lett.* **84**, 5261 (2004).
  - <sup>8</sup> W. Prellier, M. P. Singh, and P. Murugavel, *J. Phys.: Condens. Matter* **17**, R803 (2005).
  - <sup>9</sup> W. Eerenstein, F. D. Morrison, J. Dho, M. G. Blamire, J. F. Scott, and N. D. Mathur, *Science* **307**, 1203a (2005).
  - <sup>10</sup> J. Wang, A. Scholl, H. Zheng, S. B. Ogale, D. Viehland, D. G. Schlom, N. A. Spaldin, K. M. Rabe, M. Wuttig, L. Mohaddes, J. Neaton, U. Waghmare, T. Zhao, and R. Ramesh, *Science* **307**, 1203b (2005).
  - <sup>11</sup> C. Ederer and N. A. Spaldin, *Phys. Rev. B* **71**, 224103 (2005).
  - <sup>12</sup> H. Béa, M. Bibes, S. Fusil, K. Bouzehouane, E. Jacquet, K. Rode, P. Bencok, and A. Barthélémy, *Phys. Rev. B* **74**, 020101(R) (2006).
  - <sup>13</sup> J. B. Neaton, C. Ederer, U. V. Waghmare, N. A. Spaldin, and K. M. Rabe, *Phys. Rev. B* **71**, 014113 (2005).
  - <sup>14</sup> P. Ravindran, R. Vidya, A. Kjekshus, H. Fjellvag, and O. Eriksson, *Phys. Rev. B* **74**, 224412 (2006).
  - <sup>15</sup> V. V. Shvartsman, W. Kleemann, R. Haumont, and J. Kreisel, *Appl. Phys. Lett.* **90**, 172115 (2007).
  - <sup>16</sup> D. Lebeugle, D. Colson, A. Forget, M. Viret, P. Bonville, J. F. Marucco, and S. Fusil, *Phys. Rev. B* **76**, 024116 (2007).
  - <sup>17</sup> D. Lebeugle, D. Colson, A. Forget, and M. Viret, *Appl. Phys. Lett.* **91**, 022907 (2007).
  - <sup>18</sup> R. Haumont, J. Kreisel, and P. Bouvier, *Phase Transitions* **79**, 1043 (2006).
  - <sup>19</sup> J. Kreisel, R. Hamont, P. Bouvier, and B. Dkhil, to be published.
  - <sup>20</sup> A. G. Gavriliuk, V. V. Struzhkin, I. S. Lyubutin, M. Y. Hu, and H. K. Mao, *JETP Lett.* **82**, 224 (2005).
  - <sup>21</sup> A. G. Gavriliuk, V. Struzhkin, I. S. Lyubutin, I. A. Trojan, M. Y. Hu, and P. Chow, *Mater. Res. Soc. Symp. Proc.* **987**, PP05-02 (2007).
  - <sup>22</sup> U. D. Venkateswaran, V. M. Naik, and R. Naik, *Phys. Rev. B* **58**, 14256 (1998).
  - <sup>23</sup> Z. Wu and R. E. Cohen, *Phys. Rev. Lett.* **95**, 037601 (2005).
  - <sup>24</sup> J. Kreisel, B. Dkhil, P. Bouvier, and J.-M. Kiat, *Phys. Rev.*

- B **65**, 172101 (2002).
- <sup>25</sup> B. Chaabane, J. Kreisel, B. Dkhil, P. Bouvier, and M. Mezouar, Phys. Rev. Lett. **90**, 257601 (2003).
  - <sup>26</sup> I. A. Kornev, L. Bellaiche, P. Bouvier, P.-E. Janolin, B. Dkhil, and J. Kreisel, Phys. Rev. Lett. **95**, 196804 (2005).
  - <sup>27</sup> S. Kamba, D. Nuzhnyy, M. Savinov, J. Sebek, J. Petzelt, J. Prokleska, R. Haumont, and J. Kreisel, Phys. Rev. B **75**, 024403 (2007).
  - <sup>28</sup> R. P. S. M. Lobo, R. L. Moreira, D. Lebeugle, and D. Colson, cond-mat/0709.0848.
  - <sup>29</sup> F. Kubel and H. Schmid, Acta Cryst. B **46**, 698 (1990).
  - <sup>30</sup> H. K Mao, J. Xu, and P.M. Bell, J. Geophys. Res. **91**, 4673 (1986).
  - <sup>31</sup> M. I. Erements and Y. A. Timofeev, Rev. Scient. Instrum. **63**, 3123 (1992).
  - <sup>32</sup> A. L. Ruoff and K. Ghandehari, in S. C. Schmidt, J. W. Shaner, G. A. Samara, and M. Ross (Eds.), High Pressure Science and Technology, pp. 1523-1525, American Institute of Physics Conference Proceedings 309, Woodbury, N.Y. (1994).
  - <sup>33</sup> F. Gervais, in *Infrared and Millimeter Waves*, edited by K. J. Button, (Academic, New York, 1983), Chap. 7, p. 279.
  - <sup>34</sup> V. M. Orera, C. Pecharromán, J. I. Peña, R. I. Merino and C. J. Serna, J. Phys.: Condens. Matter **10**, 7501 (1998).
  - <sup>35</sup> N. W. Ashcroft and N. D. Mermin, Solid State Physics, Harcourt Brace College Publishers, Fort Worth (1976).
  - <sup>36</sup> F. Birch, J. Geophys. Res. **83**, 1257 (1978); W. B. Holzapfel, Rep. Prog. Phys. **59**, 29 (1996).
  - <sup>37</sup> P. Hermet, M. Goffinet, J. Kreisel, and Ph. Ghosez, Phys. Rev. B **75**, 220102(R) (2007).
  - <sup>38</sup> R. Haumont, J. Kreisel, P. Bouvier, and F. Hippert, Phys. Rev. B **73**, 132101 (2006).
  - <sup>39</sup> H. Fukumura, S. Matsui, H. Harima, T. Takahashi, T. Itoh, K. Kisoda, M. Tamada, Y. Noguchi, and M. Miyayama, J. Phys.: Condens. Matter **19**, 365224 (2007).
  - <sup>40</sup> P. Fischer, M. Polomska, I. Sosnowska, and M. Szymanski, J. Phys. C: Sol. Stat. Phys. **13**, 1931 (1980).
  - <sup>41</sup> P. Lunkenheimer, T. Rudolf, J. Hemberger, A. Pimenov, S. Tachos, F. Lichtenberg, and A. Loidl, Phys. Rev. B **68**, 245108 (2003).
  - <sup>42</sup> J. T. Last, Phys. Rev. **105**, 1740 (1957).
  - <sup>43</sup> M. K. Singh, S. Ryu, and H. M. Jang, Phys. Rev. B **72**, 132101 (2005).
  - <sup>44</sup> G. Xu, H. Hiraka, G. Shirane, J. Li, J. Wang, and D. Viehland, Appl. Phys. Lett. **86**, 182905 (2005).
  - <sup>45</sup> M. N. Iliev, M. V. Abrashev, H.-G. Lee, V. N. Popov, Y. Y. Sun, C. Thomsen, R. L. Meng, and C. W. Chu, Phys. Rev. B **57**, 2872 (1998).
  - <sup>46</sup> S. Frank, C. A. Kuntscher, I. Loa, K. Syassen, and F. Lichtenberg, Phys. Rev. B **74**, 054105 (2006).